Synthesis and Photoluminescence Property of Polyacetylenes Containing Liquid Crystalline Side Groups

Ching-Hua Ting and Chain-Shu Hsu*

Department of Applied Chemistry, National Chiao Tung University, Hsinchu 300, Taiwan, ROC

Received May 8, 2001; Revised May 25, 2001; Accepted May 28, 2001

Abstract: A series of new side-chain liquid crystalline (LC) polyacetylenes containing 4-(*trans*-*n*-alkylcyclohexanylcarbonyloxy)phenyl 4-alkynyloxybenzoate side groups were synthesized by using $[Rh(nbd)Cl]_2$, WCl_6 and $MoCl_5$ as polymerization catalysts. The synthesized polymers were characterized by differential scanning calorimetry, optical microscopy and X-ray diffraction measurements. The monomers showed a nematic phase while all polymers revealed the nematic, smectic A and smectic C phases. X-ray diffraction measurements proved that all the polymers show an interdigitated bilayer structure. The optical properties of the polymers were investigated by UV-vis and photoluminescent spectroscopies. The polymer films emitted green-blue photoluminescence at about 500 nm.

Keywords: Poly(acetylene), Liquid crystalline polymer, Mesomorphic property, Photoluminescence property.

Introduction

Side-chain liquid crystalline polymers (LCPs) are of both theoretical and practical interest because they combine the anisotropic properties of liquid crystals with polymeric properties and have the potential of being used for some new applications [1]. So far, most of the side-chain LCPs have been prepared mainly by radical polymerization of (meth) acrylates and by the hydrosilation of poly(methylhydrosiloxane) backbones with mesogenic olefins. In recent years, an increasing amount of research has been directed at synthesizing new well-defined side-chain LCPs by ring-opening polymerization [2-9] and living ring-opening methathesis polymerization [10-14].

Polyacetylene is the simplest class of conducting polymers. In 1993, Shirakawa et al. reported the first side-chain liquid crystalline polyacetylene prepared by Ziegler-Natta and methathesis catalysts [15-19]. Forming a liquid crystalline phase for the conducting polymer is the primary goal for the introduction of a mesogenic moiety as a substituted group in polyacetylene. The Japanese group successfully aligned the polymers using a magnetic field and found that the electrical conductivity of an aligned LC polyacetylene increased about two orders of magnitude in the direction parallel to the magnetic field [16]. The limitation on the synthesis of liquid crystalline polyacetylene is mainly due to the polar functional groups, which may poison the transition-metal catalysts. Recently, Tang et al. have developed a variety of functionality-tolerant and air and moisture-stable catalyst systems and synthesized several series of side-chain LC polyacetylenes containing mesogenic pendants with ether, ester, amide and cyano functionalties [20-24].

In this study, a series of side-chain LC poly (acetylenes) containing 4-(*trans*-*n*-alkylcyclohexanylcarbonyloxy)phenyl 4-alkynyloxybenzoate side groups are synthesized and characterized. Besides mesomorphic behavior, the photoluminescence properties of the obtained polymers are discussed.

*To whom all correspondence should be addressed.
Tel: 886-3-5712121 ext 56523; Fax: 886-3-5723764
E-mail: cshsu@cc.nctu.edu.tw

J. Polym. Res. is covered in ISI (CD, D, MS, Q, RC, S), CA, EI, and Polymer Contents.

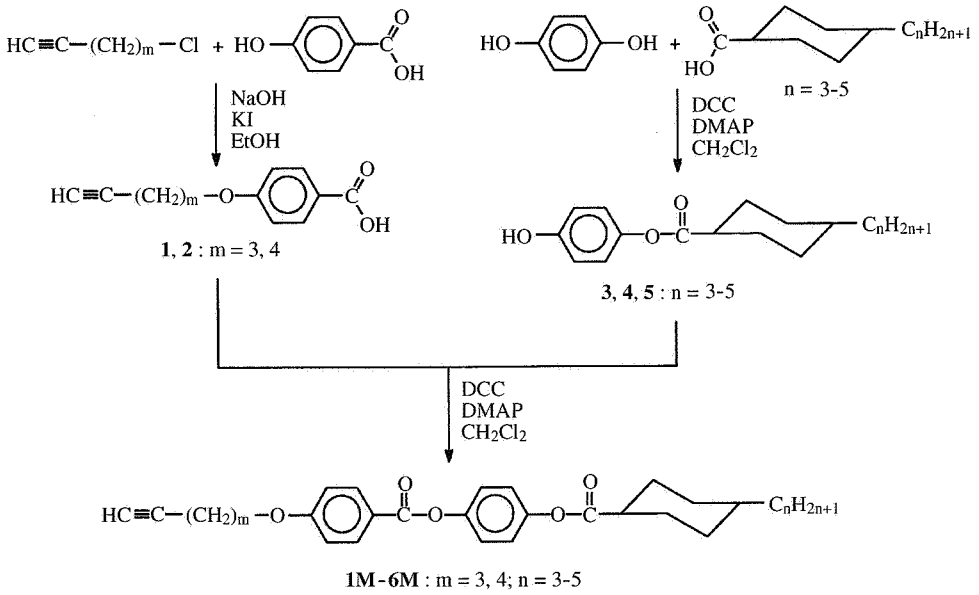

Scheme 1. Synthesis of cyclohexane- based monomers **1M-6M**.

Experimental

1. Materials

Trans-4-*n*-propylcyclohexanoic acid, *trans*-4-*n*-butylcyclohexanoic acid and *trans*-4-*n*-pentylcyclohexanoic acid were obtained from Tokyo Kasei Inc. and were used as received. Except for chloronorbornadiene rhodium (I) dimer ($[Rh(nbd)Cl]_2$, Strem), all other reagents were purchased from Aldrich and used without further purification. THF was dried over sodium, while dioxane and DMF were dried over calcium hydride before distillation.

2. Techniques

^{1}H NMR spectra (300 MHz) were recorded on a Varian VXR-300 spectrometer. Thermal transitions and thermodynamic parameters were determined by using a Seiko SSC/5200 differential scanning calorimeter equipped with a liquid nitrogen cooling accessory. Heating and cooling rate were 10 °C/min. A Nikon Microphot-FT optical polarized microscope equipped with a Mettler FP82 hot stage and a FP80 central processor was used to observe the thermal transitions and to analyze the anisotropic textures. The molecular weights of the obtained polymers were determined by GPC using a Viscotek T50A Differential Viscometer and LR125 Laser Refractometer with THF as the eluent solvent and with a polystyrene standard. The UV-Visible spectra and photoluminescence of polymers were obtained from a Shimadzu UV-1601 spectrophotometer and RF-5301PC spectrofluorophotometer, respectively.

3. Synthesis of monomers 1M-6M

The synthesis of cyclohexane containing monomers **1M-6M** is outlined in Scheme 1.

3.1 4-(4-Pentyn-1-yloxy)benzoic acid (**1**) and 4-(5-hexyn-1-yloxy)benzoic acid (**2**)

Both compounds were prepared by etherification of 5-chloro-1-pentyne or 6-chloro-1-hexyne with 4-hydroxybenzoic acid. The synthesis of compound **1** is described below.

4-Hydroxybenzoic acid (5.61 g, 40.60 mmol), NaOH (4.06 g, 101.60 mmol) and a catalytic amount of KI were dissolved in ethanol (100 mL) under gentle heating and stirring. After the introduction of 5-chloro-1-pentyne (5.00 g, 48.75 mmol), the resulting mixture was heated to reflux and stirred for 24 h. The solution was then poured into 350 mL of water and acidified with 20 mL of 37 % HCl aqueous solution. The crude product was isolated by filtration and recrystallized from 96 % methanol to yield 6.20 g (75.6 %) white crystals, mp = 149.2 °C. ^{1}H NMR ($CDCl_3$, δ, ppm): 1.97 (s, 1H, –C≡C<u>H</u>), 2.02 (m, 2H, –C<u>H$_2$</u>–), 2.41 (m, 2H, –C<u>H$_2$</u>–C≡), 4.13 (t, 2H, –OC<u>H$_2$</u>–), 6.95 and 8.02 (dd, 4H, aromatic protons).

3.2 4-Hydroxyphenyl *trans*-4-*n*-alkylcyclohexanoate (**3-5**)

Compounds **3-5** were all synthesized by the same method. The preparation of compound **4** is described below.

Trans-4-*n*-butylcyclohexanoic acid (5.00 g, 29.40 mmol), hydroquinone (8.08 g, 73.40 mmol) and *N*,*N*-dimethylaminopyridine (DMAP, 0.36 g,

2.93 mmol) were dissolved in dry CH_2Cl_2 (120 mL) under an N_2 atmosphere. The solution was cooled to 0 °C and dicyclohexyl carbodiimide (DCC, 7.27 g, 35.2 mmol) in 30 mL of dry CH_2Cl_2 was added dropwise. The reaction mixture was stirred at room temperature for 14 h and filtered. The crude product, which was isolated by evaporating the solvent, was purified by column chromatography (silica gel, ethyl acetate/*n*-hexane = 1/5 as eluent) and finally recrystallized from methanol to yield 4.95 g (65.8 %) of white crystals, mp = 90.3 °C. ^1H NMR ($CDCl_3$, δ, ppm): 0.86 (t, 3H, $-C\underline{H}_3$), 0.90-2.41 (m, 17H, cyclohexane and terminal alkyl group $-(C\underline{H}_2)_3-$), 5.31 (s, 1H, $-O\underline{H}$), 6.79 and 6.87 (dd, 4H, aromatic protons).

3.3 4-(*Trans*-4-*n*-alkylcyclohexanyloxy)phenyl 4-(4-pentyn-1-yloxy)benzoate (**1M-3M**, n = 3-5), and 4-(*trans*-4-*n*-alkylcyclohexanyloxy)phenyl 4-(5-hexyn-1-yloxy)benzoate (**4M-6M**, n = 3-5)

Monomers **1M-6M** were synthesized by the same esterification of compounds **3-5** with 4-(4-pentyn-1-yloxy)benzoic acid or 4-(5-hexyn-1-yloxy) benzoic acid. The preparation of monomer **2M** is described below.

4-(4-Pentyn-1-yloxy)benzoic acid (1.00 g, 4.90 mmol), 4-hydroxyphenyl *trans*-4-*n*-butylcyclohexanoate (1.29 g, 4.90 mmol) and *N*,*N*-dimethylaminopyridine (DMAP, 0.06 g, 0.49 mmol) were disolved in dry CH_2Cl_2 (70 mL) under an N_2 atmosphere. The solution was cooled to 0 °C and dicyclohexyl carbodiimide (DCC, 1.52 g, 7.35 mmol) in 20 mL of dry CH_2Cl_2 was added dropwise. The reaction mixture was stirred at room temperature for 14 h and filtered. The crude product, which was isolated by evaporating the solvent, was purified by column chromatography (silica gel, ethyl acetate/*n*-hexane = 1/1 as eluent) and finally recrystallized from methanol to yield 1.65 g (76%) of white crystals, mp = 150.9 °C. Detailed characterization data and the yield of monomers **1M-6M** are summarized in Table I.

4. Polymerization of monomers 1M-6M

Scheme 2 outlined the polymerization of monomers **1M-6M**. All the polymerization reactions and manipulations were carried out under nitrogen using either an inert-atmosphere glovebox or the Schlenk technique in a vacuum line system, except for the purification of the polymers, which was performed in an open atmosphere. The experimental procedures for the polymerization of monomer **2M** are given below.

Monomer **2M** (0.37 g, 0.80 mmol) was added into a Schlenk tube with a three-way stopcock on the side arm. The tube was evacuated under a vacuum and then flushed with dried N_2 three times through the side arm. A mixture of dioxane and THF (4/1 by volume, 2 mL) was injected into the tube through a septum to dissolve the monomer. The catalyst solution was prepared in another tube by dissolving WCl_6 (31.72 mg, 0.08 mmol) and Ph_4Sn (34.16 mg, 0.08 mmol) in 2 mL of the same mixture solvent. Both tubes were aged at room temperature for 30 min. The monomer solution was then transferred to the catalyst solution using a hypodermic syringe. The reaction mixture was stirred at 80 °C under N_2 for 24 h. The solution was then cooled to room temperature, diluted with 2 mL of THF and added dropwise to 300 mL of methanol through a cotton filter with stirring. The polymers were separated by filtration, purified by several reprecipitations from THF into methanol and dried in a vacuum oven.

Results and Discussion

1. Polymerization reaction

Mo-, W- and Rh-based catalysts are the most widely used initiators for the polymerization of acetylene-based monomers [15-24]. Tang et al. found that WCl_6-Ph_4Sn/dioxane was the best catalyst system for the polymerization of acetylene-based monomers with polar functionalities [21]. In this study, monomers **1M-6M** belong to acetylene-based monomers, therefore, we chose WCl_6, $MoCl_5$ and $[Rh(nbd)Cl]_2$ as catalysts and Ph_4Sn as a cocatalyst. Table II lists the polymerization results of monomer **2M**. When WCl_6 was used as the catalyst and Ph_4Sn was used as the cocatalyst, no polymerization occurred in dioxane at room temperature. When the polymerization temperature was raised to 80 °C, the polymerization still proceeded but the yield was very low (11.9 %). When THF was used as the cosolvent, the yield was improved because the solubility of the monomer was greatly enhanced. With $MoCl_5$/Ph_4Sn as the catalyst system, no polymerization occurred at room temperature again. When the reaction temperature was raised to 80 °C, a higher yield was obtained. However, the molecular weight of the obtained polymer was very low ($\overline{M}_w$ = 1,300). In the case of $[Rh(nbd)Cl]_2$, polymerization occurred at room temperature. When the polymerization temperature was raised to 80 °C, the yield decreased. Therefore, we chose the following polymerization conditions for other monomers: (i) WCl_6-Ph_4Sn used as catalyst, (ii) a mixture of dioxane and THF used as solvent, (iii) polymerization at 80 °C. Table III reports the polymerization results of monomers **1M-6M**. All polymerizations give poly-

Table I. Characterization of monomers **1M-6M**.

Monomer	Yield (%)	300 MHz ^{1}H NMR ($CDCl_3$, δ, ppm)
1M	76	0.87 (t, 3H, $-C\underline{H}_3$), 1.97 (s, 1H, $\underline{H}C\equiv C-$), 0.91-2.32 (m, 17H, $-C\equiv C-(C\underline{H}_2)_2-$ and $-(C\underline{H}_2)_2-C\underline{H}$ ), 2.43 (m, 1H, 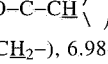), 4.15 (t, 2H, $-OC\underline{H}_2-$), 6.98-8.10 (two dd, 8H, aromatic protons)
2M	75.8	0.88 (t, 3H, $-C\underline{H}_3$), 1.97 (s, 1H, $\underline{H}C\equiv C-$), 0.90-2.33 (m, 19H, $-C\equiv C-(C\underline{H}_2)_2-$ and $-(C\underline{H}_2)_3-C\underline{H}$ 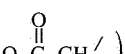), 2.43 (m, 1H, 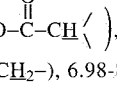), 4.12 (t, 2H, $-OC\underline{H}_2-$), 6.98-8.10 (two dd, 8H, aromatic protons)
3M	66	0.89 (t, 3H, $-C\underline{H}_3$), 1.97 (s, 1H, $\underline{H}C\equiv C-$), 0.91-2.33 (m, 21H, $-C\equiv C-(C\underline{H}_2)_2-$ and $-(C\underline{H}_2)_4-C\underline{H}$ 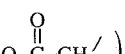), 2.43 (m, 1H, 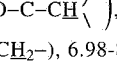), 4.15 (t, 2H, $-OC\underline{H}_2-$), 6.98-8.10 (two dd, 8H, aromatic protons)
4M	78	0.87 (t, 3H, $-C\underline{H}_3$), 1.97 (s, 1H, $\underline{H}C\equiv C-$), 0.91-2.35 (m, 19H, $-C\equiv C-(C\underline{H}_2)_3-$ and $-(C\underline{H}_2)_2-C\underline{H}$ ), 2.45 (m, 1H, 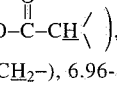), 4.06 (t, 2H, $-OC\underline{H}_2-$), 6.96-8.09 (two dd, 8H, aromatic protons)
5M	69	0.88 (t, 3H, $-C\underline{H}_3$), 1.97 (s, 1H, $\underline{H}C\equiv C-$), 0.91-2.35 (m, 21H, $-C\equiv C-(C\underline{H}_2)_3-$ and $-(C\underline{H}_2)_3-C\underline{H}$ 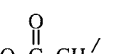), 2.45 (m, 1H, 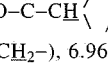), 4.06 (t, 2H, $-OC\underline{H}_2-$), 6.96-8.10 (two dd, 8H, aromatic protons)
6M	72	0.87 (t, 3H, $-C\underline{H}_3$), 1.97 (s, 1H, $\underline{H}C\equiv C-$), 0.91-2.35 (m, 23H, $-C\equiv C-(C\underline{H}_2)_3-$ and $-(C\underline{H}_2)_4-C\underline{H}$ 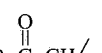), 2.45 (m, 1H, 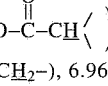), 4.06 (t, 2H, $-OC\underline{H}_2-$), 6.96-8.10 (two dd, 8H, aromatic protons)

mers with reasonably high yields and molecular weights.

2. Structure characterization of polymers 2P

Figure 1 presents the comparison of IR spectra of monomer **2M** and its corresponding polymer **2P**. The monomer absorbs at about 3303 and 2115 cm^{-1}, due respectively to the ≡C–H stretching and C≡C stretching vibrations. The acetylene absorption bands disappear in the spectra of the polymer and a new double bond absorption at 3073 cm^{-1} appears in the polymer spectra, confirming that acetylene triple bonds have been transferred to conjugated double bonds during polymerization.

Figure 2 shows the ^{1}H NMR spectra of monomer **2M** and polymers **2P**. In the spectra of polymer **2P**, the acetylene proton peak at 1.97 ppm disappears and all other peaks become broad. A new peak is observed at 6.09 ppm. According to Tang et al. [21], the chemical shift of the *cis*-olefin proton appears at the region of 5.88-6.26 ppm for mesogen-containing poly(1-alkynes). Therefore, we can assign the peak at 6.09 ppm as the *cis*-olefin proton and calculate the *cis*-content of the polymer by the following equation:

Table II. Polymerization of 4-(*trans*-4-*n*-butylcyclohexanyloxy)phenyl 4-(4-pentyn-1-yloxy)benzoate (**2M**)[a].

No.	Catalyst	Solvent	Reaction temp. (°C)	Yield (%)	$\overline{M_w}$[b]	$\overline{M_w}/\overline{M_n}$[b]	*Cis*- content[c]
1	WCl_6/Ph_4Sn	Dioxane	r.t.	0	–	–	–
2	WCl_6/Ph_4Sn	Dioxane	80	11.9	41300	1.24	0
3	WCl_6/Ph_4Sn	Dioxane/THF = 4/1[d]	80	87.3	69500	1.31	0
4	$MoCl_5/Ph_4Sn$	Dioxane/THF = 4/1[d]	r.t.	0	–	–	–
5	$MoCl_5/Ph_4Sn$	Dioxane/THF = 4/1[d]	80	78.2	1300	1.15	0
6	$[Rh(nbd)Cl]_2$	DMF/Et_3N = 4/1[d]	r.t.	41.0	22320	1.73	37.4
7	$[Rh(nbd)Cl]_2$	DMF/THF/Et_3N = 3/1/1[d]	r.t.	88.4	11390	1.41	43.0
8	$[Rh(nbd)Cl]_2$	DMF/THF/Et_3N = 3/1/1[d]	80	71.7	7310	1.46	0

(a) Carried out under nitrogen for 24 h; $[M]_0$ = 0.2 M, $[[Rh(nbd)Cl]_2]$ = 10 mM, $[WCl_6]$ = $[MoCl_5]$ = $[Ph_4Sn]$ = 20 mM; nbd = 2,5-norborndiene, Ph_4Sn = tetraphenyltin.
(b) Determined by GPC in THF on the basis of a polystyrene calibration.
(c) *Cis*-content in polymer sample.
(d) Volume ratio.

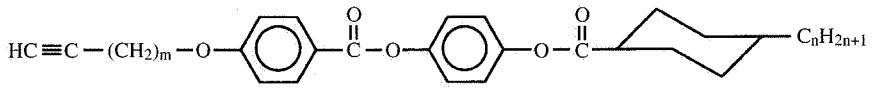

1M-6M : m= 3, 4; n = 3-5

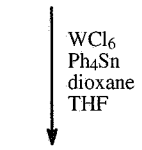

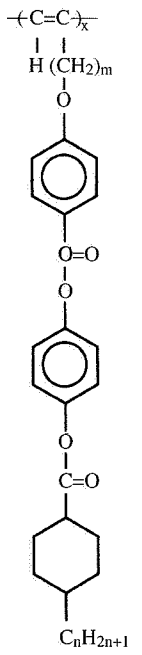

1P-6P : m = 3, 4; n = 3-5

Scheme 2. Synthesis of side-chain LC polyacetylene **1P-6P**.

$$\textit{cis}\text{-content (\%)} = \{A_{6.09}/[(A_{7.89}+A_{6.97}+A_{6.72}+A_{6.09})/9]\} \times 100 \quad (1)$$

The *cis*-contents of all polymers are listed in Tables II and III. We found that the *cis*-content depended on the polymerization catalyst. When $[Rh(nbd)Cl]_2$ was used as the catalyst, the *cis*-content of the ob-

Table III. Polymerization of monomers **1M-6M**[a].

Monomer	Yield (%)	*Cis*-content[b]	$\overline{M_n}$[c]	$\overline{M_w}$[c]	$\overline{M_w}/\overline{M_n}$[c]
1M	81.9	0	42100	67600	1.61
2M	87.3	0	53100	69500	1.31
3M	79.9	0	40100	77300	1.93
4M	76.2	0	64300	106600	1.66
5M	86.7	0	57200	108900	1.90
6M	69.7	0	44200	56800	1.29

(a) Polymerization in dioxane/THF mixture solvent (volume ratio of THF to dioxane was 1/4) at 80 °C under nitrogen for 24 h; $[M]_0$ = 0.2 M, $[WCl_6]$ = $[Ph_4Sn]$ = 20 mM.
(b) *Cis*-content in polymer sample.
(c) Determined by GPC in THF on the basis of a polystyrene calibration.

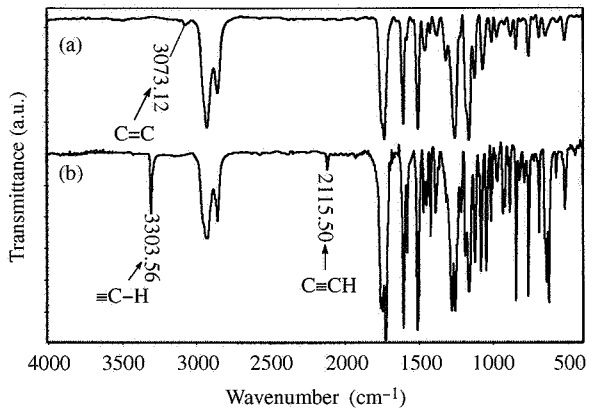

Figure 1. IR spectra of (a) monomer **2M** and (b) polymer **2P**.

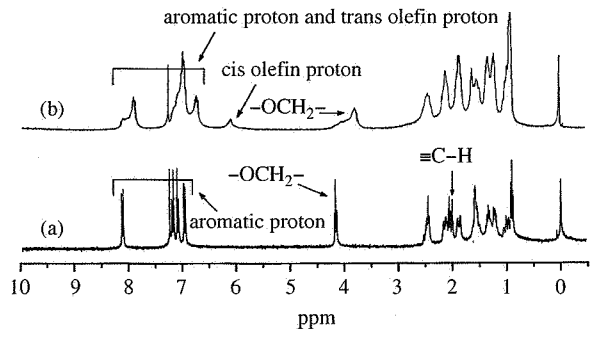

Figure 2. ^{1}H NMR spectra of (a) monomer **2M** and (b) polymer **2P**.

tained polymer was around 40 %. However, when WCl_6 was used as the catalyst, the polymers contained 100 % of *trans*-olefin in the polyacetylene backbones.

3. Mesomorphic properties of polymers 1P-6P

The thermal behavior of all monomers is reported in Table IV. All monomers reveal an enantiotropic nematic phase. When we consider the

Table IV. Thermal transitions and thermodynamic parameters of monomers **1M-6M**.

Monomer	m[a]	n[a]	Phase Transitions, °C (Corresponding Enthalpy Changes, Kcal/mol)[b] Heating / Cooling
1M	3	3	K 150.5(8.55) N 225.5(0.47) I / I 223.3(0.44) N 107.3(7.77) K
2M	3	4	K 150.9(8.63) N 219.2(0.24) I / I 216.5(0.40) N 113.9(8.10) K
3M	3	5	K 129.7(8.76) N 204.9(0.32) I / I 207.9(0.35) N 99.9(7.92) K
4M	4	3	K 110.9(9.43) N 211.2(0.44) I / I 206.2(0.29) N 72.4(8.49) K
5M	4	4	K 99.2(5.99) N 203.8(0.23) I / I 201.4(0.28) N 74.5(5.70) K
6M	4	5	K 99.8(8.09) N 181.5(0.14) I / I 175.5(0.11) N 66(7.69) K

(a) According to Scheme 1.
(b) K = crystalline, N = nematic, I = isotropic.

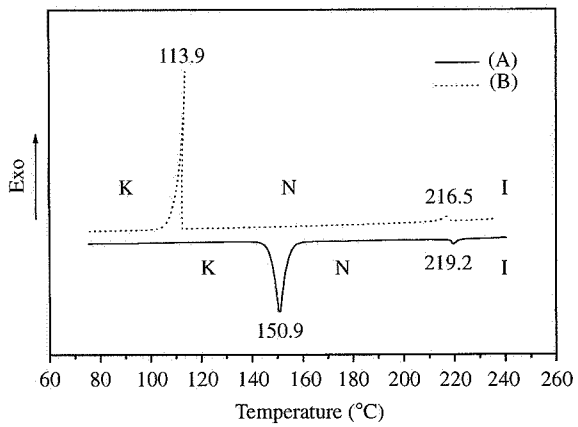

Figure 3. DSC thermogram of monomer **2M** (10 °C/min): (a) heating scan and (b) cooling scan.

spacer effect, we find that the melting points decrease gradually as the spacer length (i.e., m value) increases. Figure 3 displays the representative DSC trace of polymer **2M**. In the heating scan, it shows a melting transition at 150.9 °C and a nematic to isotropic phase transition at 219.0 °C. The cooling scan shows a very similar phase behavior, except that the crystalization temperature has 37 °C supercooling.

Table V summarizes the phase transitions of polymers **1P-6P**. All polymers reveal nematic, smectic A and smectic C phases. Mesophase identification has been accomplished by DSC measure-ment, optical polarizing microscopic observation and X-ray diffraction. Figure 4 presents the representative

Table V. Thermal transitions of liquid crystalline polyacetylenes **1P-6P**.

Polymer	m[a]	n[a]	Phase transitions (°C)[b]
1P	3	3	G 58.4 S_C 216.2 S_A (285)[c] N (291)[c] I 309.8 decomposed
2P	3	4	G 62.3 S_C 202.0 S_A (298)[c] N (310)[c] I 328.3 decomposed
3P	3	5	G 63.3 S_C 188.7 S_A (297)[c] N (302)[c] I 322.0 decomposed
4P	4	3	G 59.3 S_C 161.5 S_A (277)[c] N (290)[c] I 299.9 decomposed
5P	4	4	G 62.3 S_C 171.0 S_A (275)[c] N (284)[c] I 294.6 decomposed
6P	4	5	G 56.0 S_C 137.4 S_A (290)[c] N (310)[c] I 311.3 decomposed

(a) According to Scheme 1.
(b) Data taken from the first heating scan. Code: G, glassy state; S_C, smectic C phase; S_A, smectic A phase; N, nematic phase; I, isotropic liquid.
(c) Phase transition temperatures obtained by optical polarizing microscopic observation.

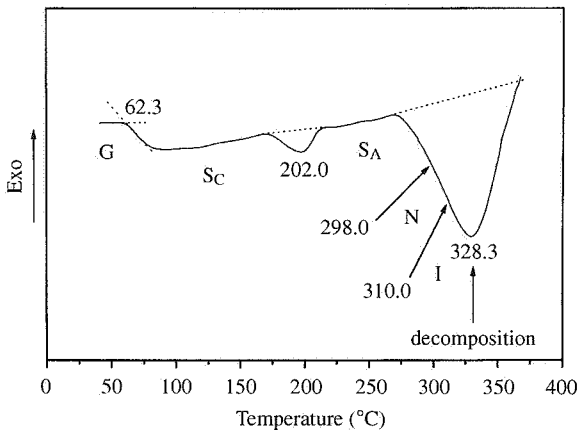

Figure 4. DSC thermogram of polymer **2P** (10 °C/min): the first heating scan.

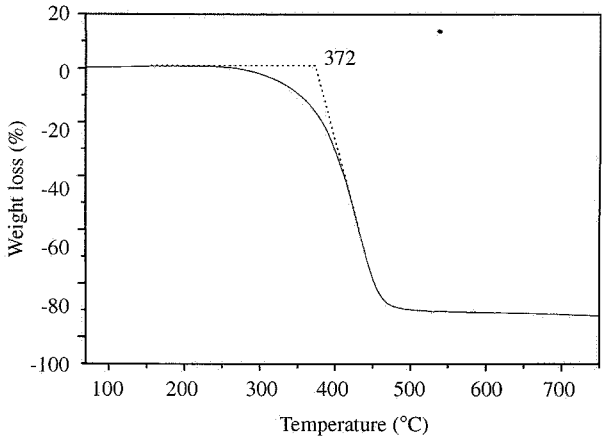

Figure 5. TGA thermogram of polymer **2P**.

DSC trace of polymer **2P**. It exhibits two endothermic peaks at 202 and 328.3 °C in the first heating scan. The optical polarizing microscope observed a smectic A to nematic phase transition at 298 °C and a nematic to isotropic phase transition at 310 °C. However both transitions were covered by a big decomposition peak. In the TGA measurement (see Figure 5), the polymer decomposed when the temperature was higher than 300 °C. Figure 6 shows the temperature-dependent X-ray diffraction diagrams obtained from powder samples of **2P** at 205 and 90 °C. Curve (a) presents a diffuse reflection at 4.60 Å, which corresponds to the lateral spacing of two mesogenic side groups, a sharp first order reflection at 40.22 Å, and a second order reflection at 20.85 Å corresponding to smectic layers. When the measuring temperature was lowered from 205 to 90 °C, the *d*-spacing of the first order reflection decreased from 40.22 to 39.65 Å (curve (b)), giving strong evidence for the formation of a tilted smectic C phase. The layer spacing was about 1.5 times the calculated length of the mesogenic side group. Therefore, we can conclude that the polymer forms

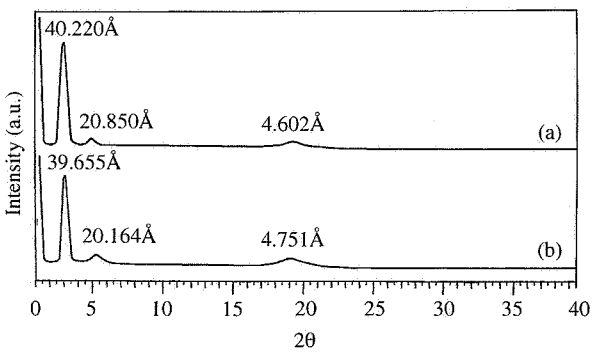

Figure 6. X-ray diffraction patterns of polymer **2P** measured at (a) 205 °C and (b) 90 °C.

a interdigitated bilayer structure (see Figure 7).

4. Photoluminescence properties of polymers 1P-6P

Table VI summarizes the results of UV-vis and photoluminescence (PL) spectra of polymers **1P-6P**. All polymers present two UV-vis absorption peaks in THF solution at about 262 and 222 nm, and the

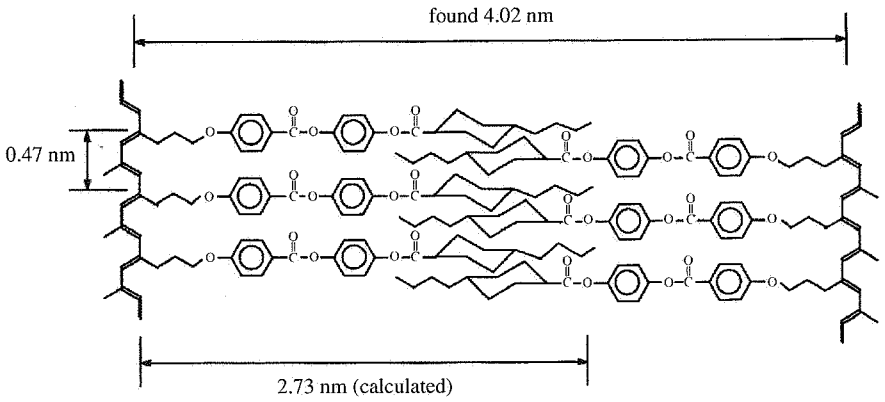

Figure 7. Smectic layer structure of polyacetylene **2P**.

Table VI. UV-visible and photoluminescence spectral data of polymers **1P-6P**.

Polymer	UV-Visible[a]		Photoluminescence[b]	
	λ_{abs} (nm)		λ_{ex} (nm)	λ_{em} (nm)
1P	265	224	265	489
2P	269	226	269	497
3P	262.5	223.5	262	488
4P	262	222.5	262	508
5P	261.5	222	261	514
6P	262.5	223.5	262	492

(a) Code: λ_{abs}, absorptive wavelength in UV-Visible spectrum.
(b) Code: λ_{ex}, exciting wavelength used in the measurement of photoluminescence; λ_{em}, emissive wavelength in photoluminescence spectrum.

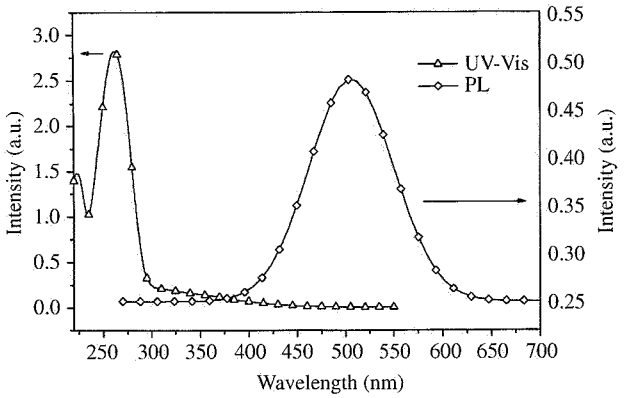

Figure 8. UV-visible (Δ) and photoluminescence (◊) spectra of polymer **2P**.

polymer films emit a PL peak near 500 nm. Figure 7 shows the representative UV-vis and PL spectra of polymer **2P**. The PL intensity of pure polymer **2P** is quite weak due to the strong interchain energy transfer between the polymer chains' aggregation [26]. Figure 8 shows the photoluminescence spectra of the blending samples of polymer **2P** and poly(methyl methacrylate) (PMMA). After introducing the PMMA to blend with polymer **2P**, the PL intensity obviously increases because the PMMA will suppress the interchain interaction of polymer **2P**.

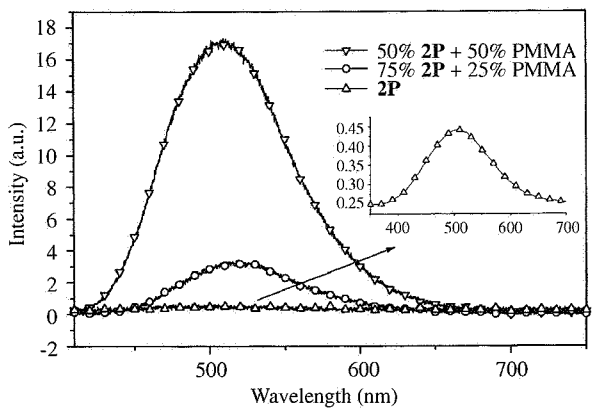

Figure 9. Photoluminescence spectra of polymer **2P** and its blends with PMMA.

Conclusion

A new series of side-chain LC polyacetylenes containing 4-(*trans-n*-alkylcyclohexanylcarbonyloxy) phenyl 4-alkynyloxybenzoate side groups were synthesized using simple metal halide catalysts. The polymers obtained by using $[Rh(nbd)Cl]_2$ as a catalyst contain about 40% *cis*-configuration in the polyacetylene backbone. When the WCl_6 was used as the catalyst, the obtained polymers contained 100 % *trans*-configuration. Polymers **1P-6P** display nematic, smectic A and smectic C phases. All polymers have a weak photoluminescence emission

at about 500 nm. After blending with PMMA, their PL intensities will largely increase.

Acknowledgments

The authors are grateful to the National Science Council of the Republic of China for financial support of this work (NSC 89-2216-E009-023).

References

1. C. S. Hsu, *Prog. Polym. Sci.*, **22**, 829 (1997).
2. P. A. Tuan, S. G. Kostromin and V. P. Shibaev, *Polym. Bull.*, **29**, 49 (1992).
3. K. Fujishiro, A. D. Pajerski and R. W. Lenz, *Liq. Cryst.*, **12**, 417 (1992).
4. K. Fujishiro and R. W. Lenz, *Liq. Cryst.*, **12**, 561 (1992).
5. P. A. Tuan, S. G. Kostromin and V. P. Shibaev, *Polym. Bull.*, **30**, 249 (1993).
6. E. Akiyama and Y. Nagase, *Makromol. Chem., Rapid. Commun.*, **14**, 251 (1993).
7. Y. Kawakami, K. Takahashi and H. Hibino, *Macromolecules*, **24**, 4531 (1991).
8. Y. Kawakami and K. Takahashi, *Polym. Bull.*, **25**, 439 (1991).
9. Y. Kawakami, K. Takahashi, S. Nishiguchi and K. Toida, *Polym. Int.*, **31**, 35 (1993).
10. Z. Komiya, C. Pugh and R. R. Schrock, *Macromolecules*, **25**, 6586 (1992).
11. C. Pugh and R. R. Schrock, *Macromolecules*, **25**, 6593 (1992).
12. Z. Komiya and R. R. Schrock, *Macromolecules*, **26**, 1387 (1993).
13. Z. Komiya and R. R. Schrock, *Macromolecules*, **26**, 1393 (1993).
14. S. H. Kim, H. J. Lee, S. H. Jin, H. N. Cho and S. K. Choi, *Macromolecules*, **26**, 846 (1993).
15. S. Y. Oh, K. Akagi, H. Shirakawa and K. Araya, *Macromolecules*, **26**, 6203 (1993).
16. H. Gato, K. Akagi, H. Shirakawa, S. Y. Oh and K. Araya, *Synth. Met.*, **71**, 1899 (1995).
17. K. Akagi and H. Shirakawa, *Macromol. Sym.*, **104**, 137 (1996).
18. K. Yoshino, K. Kobayashi, K. Myojin, M. Ozaki, K. Akagi, H. Gato and H. Shirakawa, *Jpn. J. Appl. Phys.*, **35**, 3964 (1996).
19. X. M. Dai, H. Gato, K. Akagi and H. Shirakawa, *Synth. Met.*, **102**, 1289 (1999).
20. B. Z. Tang, X. Kong, X. Wan and X. D. Feng, *Macromolecules*, **30**, 5620 (1997).
21. B. Z. Tang, X. Kong, X. Wan, H. Peng, W. Y. Lam, X. D. Feng and H. S. Kwok, *Macromolecules*, **31**, 2419 (1998).
22. X. Kong and B. Z. Tang, *Chem. Mater.*, **10**, 3352 (1998).
23. X. Kong, W. Y. Lam and B. Z. Tang, *Macromolecules*, **32**, 1722 (1999).
24. W. Y. Lam, X. Kong, Y. Dong, K. L. Cheuk, K. Xu and B. Z. Tang, *Macromolecules*, **33**, 5027 (2000).
25. T. J. Katz and S. J. Lee, *J. Am. Chem. Soc.*, **102**, 422 (1980).
26. K. Yoshino, M. Hirohata, R. Hidayat, K. Tada, T. Sada, M. Teraguchi, T. Masuda, S. V. Frolov, M. Shkunov, Z. V. Vardeny and M. Hamaguchi, *Synth. Met.*, **91**, 283 (1997).